





Complex evolution of the magnetic transitions and unexpected absence of bulk superconductivity in chemically precompressed NaMn_6Bi_5

P. F. Shan ^{1,2,*}, Q. X. Dong,^{1,2,*} P. T. Yang,^{1,2} L. Xu,^{1,2} Z. Y. Liu,^{1,2} L. F. Shi,^{1,2} N. N. Wang,^{1,2} J. P. Sun ^{1,2},
Y. Uwatoko,³ G. F. Chen,^{1,2,†} B. S. Wang ^{1,2,†} and J.-G. Cheng ^{1,2,†}

¹Beijing National Laboratory for Condensed Matter Physics and Institute of Physics, Chinese Academy of Sciences, Beijing 100190, China

²School of Physical Sciences, University of Chinese Academy of Sciences, Beijing 100190, China

³Institute for Solid State Physics, University of Tokyo, Kashiwa, Chiba 277-8581, Japan



(Received 12 December 2022; revised 17 March 2023; accepted 20 March 2023; published 29 March 2023)

Pressurized AMn_6Bi_5 ($A = \text{K, Rb, Cs}$) members have recently emerged as a new family of ternary manganese-based superconductors that exhibits a broad superconducting dome with a maximum critical temperature up to ~ 9.5 K adjacent to the long-range antiferromagnetic phase in their T - P phase diagrams. The analogous compound NaMn_6Bi_5 , with a smaller A -site cation and lower antiferromagnetic transition temperatures $T_1 \approx 46$ K and $T_2 \approx 52$ K is expected to show superconductivity at lower pressures. By performing detailed high-pressure electrical transport measurements on the chemically precompressed NaMn_6Bi_5 single crystals, we map out the complex evolution with pressure of its multiple magnetic transitions, which are eventually suppressed by pressures. Contrary to the expectation, the bulk superconductivity is absent near the magnetic quantum critical point, where we observed a weak decrease in resistance below 2.4 K in a narrow pressure range of 12 to 14.4 GPa from the measurements in a diamond anvil cell. The origin of this anomaly remains unclear, and it might be ascribed to the presence of filamentary superconductivity in analogy to other AMn_6Bi_5 . These distinct results of NaMn_6Bi_5 with respect to other AMn_6Bi_5 members highlight the complexity of magnetism and its interplay with superconductivity in this family of quasi-one-dimensional compounds.

DOI: [10.1103/PhysRevB.107.094519](https://doi.org/10.1103/PhysRevB.107.094519)

I. INTRODUCTION

The 3d transition-metal-based compounds with narrow bands usually possess strong electron correlations and are close to magnetic instability, putting them at the forefront of exploring unconventional superconductivity (SC) [1–3]. The enhanced magnetic fluctuations brought by adjusting lattice dimensionality and/or the destabilization of magnetic orders have been considered an important glue for forming Cooper pairs [2–15]. The celebrated examples include the cuprates [1,3] and iron-based high-critical temperature (T_c) superconductors [4–8], as well as the two-dimensional triangular lattice Na_xCoO_2 [9,10]. By following these strategies, we discovered SC in pressurized CrAs and MnP on the border of their helimagnetic orders [13,16]. These discoveries have motivated researchers to explore more chromium- and manganese-based superconductors, leading to the recent discoveries of several new chromium-based superconducting materials, including $\text{A}_2\text{Cr}_3\text{As}_3$ ($A = \text{Na, K, Rb, Cs}$) [17–20], ACr_3As_3 ($A = \text{K, Rb}$) [21,22], and $\text{R}_3\text{Cr}_{10-x}\text{N}_{11}$ ($R = \text{La, Pr}$) [23,24]. All these new chromium-based superconductors exhibit intriguing physical properties at ambient pressure (AP). However, progress on the manganese-based superconductors is rather stagnant, and only the high-pressure (HP) orthorhombic phase of MnSe was very recently found to show SC above 15 GPa [25]. Many three-dimensional manganese-based an-

tiferromagnetic (AFM) materials have been found to show structural/magnetic instability at some critical pressures, but without SC (e.g., Mn_3P [26] and $\alpha\text{-Mn}$ [27,28]). The reduction of lattice dimension that often weakens magnetic orders and enhances spin fluctuations [29,30] can be taken as an alternative means for finding more manganese-based superconductors.

Indeed, pressure-induced SC with a relatively high T_c of ~ 9.5 K has been achieved recently in the ternary AMn_6Bi_5 ($A = \text{K, Rb, and Cs}$) with a quasi-one-dimensional (Q1D) structure [31–33]. As illustrated in Fig. 1(a), the crystal structure is featured by parallel infinite $[\text{Mn}_6\text{Bi}_5]^-$ chains formed by an alternating arrangement of Mn_{10} and Bi_{10} pentagons with an additional Mn-atom chain in the core; the nearest manganese and bismuth atoms constitute face-shared pentagonal antiprisms. All these compounds show metallic conductivity and undergo long-range AFM transition at the transition temperatures of $T_N = 75, 83,$ and 87 K for $A = \text{K, Rb, and Cs}$, respectively. According to the single-crystal neutron diffraction results on KMn_6Bi_5 [34], its AFM structure is characterized as a complex transverse incommensurate spin density wave with quite a large periodicity along the b -axis. When these Q1D AFM metals are subjected to hydrostatic pressures, the superconducting state is found to emerge above some critical pressure P_c , where the AFM order just vanishes, i.e., a broad superconducting dome appears adjacent to the AFM phase. For these three compounds, their T - P phase diagrams in terms of the values of $P_c \approx 12$ to 13 GPa and the optimal $T_c \approx 9$ K are quite similar. In addition, unconventional SC with a multiband character has been inferred

*These authors contributed equally to this work.

†gfchen@iphy.ac.cn, bswang@iphy.ac.cn, jgcheng@iphy.ac.cn

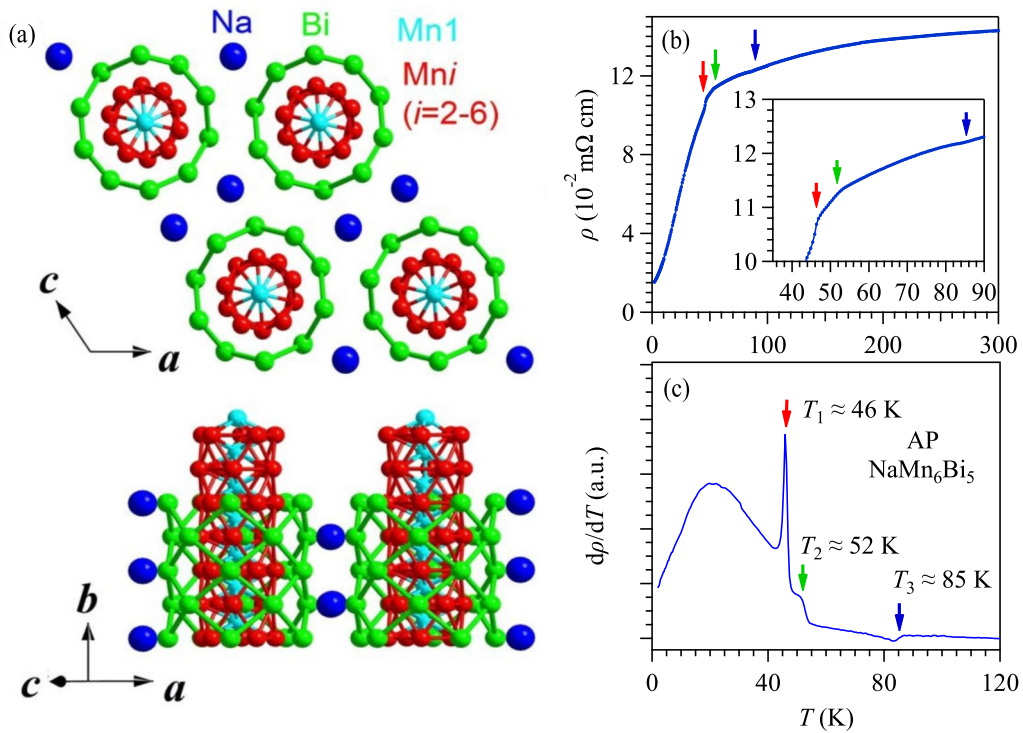


FIG. 1. (a) Crystal structure of quasi-one-dimensional NaMn₆Bi₅ parallel and perpendicular to the *b*-axis. (b) Temperature dependence of resistivity (1.5 to 300 K). (c) The derivative $d\rho/dT$ at AP. Three phase transitions are marked by the arrows.

from the available results, i.e., the observations of large upper critical fields beyond the Pauli paramagnetic limit and a deviation from the fittings with the single-band Ginzburg-Landau theory [31,32,35]. This new discovery reignites interest in the manganese-based superconductors, and systematic studies of AMn₆Bi₅ are valuable to get more insights into the pairing mechanism of unconventional SC.

In addition to AMn₆Bi₅ ($A = \text{K, Rb, Cs}$), a new analogous compound, NaMn₆Bi₅, with a smaller *A*-site cation was recently synthesized and found to display some peculiar physical properties at AP [36]. For example, it undergoes multiple phase transitions, including two successive AFM-like transitions at $T_1 \approx 47$ K and $T_2 \approx 52$ K, and a third transition at $T_3 \approx 85$ K with unknown origin. By contrast, the other AMn₆Bi₅ exhibits a single AFM phase transition, as mentioned earlier. In addition, an unusually large Sommerfeld coefficient, $\gamma = 139.13$ mJ mol⁻¹ K⁻² was observed in NaMn₆Bi₅ and has been attributed to the enhanced density of states near the Fermi level according to density functional theory calculations [36]. As a chemically precompressed analogy of AMn₆Bi₅ with lower AFM phase transition temperatures, NaMn₆Bi₅ is expected to be a promising superconducting parent compound with possible lower P_c .

The purpose of this work is thus to investigate the pressure effect on the transport properties of NaMn₆Bi₅ with an aim to find SC and to achieve a more comprehensive understanding of the mechanisms of pressure-induced SC in the family of AMn₆Bi₅. The evolution of multiple phase transitions in the low-pressure range is determined through detailed transport measurements. Different from the other members (K/Rb/Cs) Mn₆Bi₅ [31–33], the obvious signatures of bulk

SC were not observed upon suppression of its AFM orders. Instead, we only observed a weak resistance drop below 2.4 K, the origin of which remains unclear at present but might be ascribed to the possible filamentary SC in analogy to other AMn₆Bi₅. The present study [31–33] together with previous work thus highlights the complexity of magnetism and its interplay with SC in this Q1D AMn₆Bi₅ family.

II. EXPERIMENTAL METHODS

NaMn₆Bi₅ single crystals were grown by adopting the Na-Bi flux as reported previously [36–38]. The obtained needle-like single crystals have the silvery metallic luster and their size can be as large as $\sim 5.0 \times 0.5 \times 0.5$ mm³. The quality of the samples was checked on a Bruker D8 single-crystal X-ray diffractometer with molybdenum K_α ($\lambda = 0.71073$ Å) at 300 K in an argon atmosphere. Our results confirm that NaMn₆Bi₅ has the monoclinic structure with a $C2/m$ (No. 12) space group, which is identical to those of (K/Rb/Cs) Mn₆Bi₅, as shown in Fig. 1(a). The chemical compositions of Na:Mn:Bi are close to the stoichiometric ones, as verified by an energy dispersive x-ray spectroscopy. Electrical resistivity, $\rho(T)$, of NaMn₆Bi₅ at AP was measured on a commercial quantum design physical property measurement system ($1.8 \text{ K} \leq T \leq 400 \text{ K}$, $0 \leq H \leq 9 \text{ T}$). Temperature dependence of resistance for NaMn₆Bi₅ under HP was first measured by using a self-clamped piston cylinder cell (PCC) under hydrostatic pressures up to 2.25 GPa. Here, the Daphne 7373 was used as the pressure transmitting medium (PTM) in the PCC. Then, measurements of resistance under pressures up to 14 GPa were performed in a

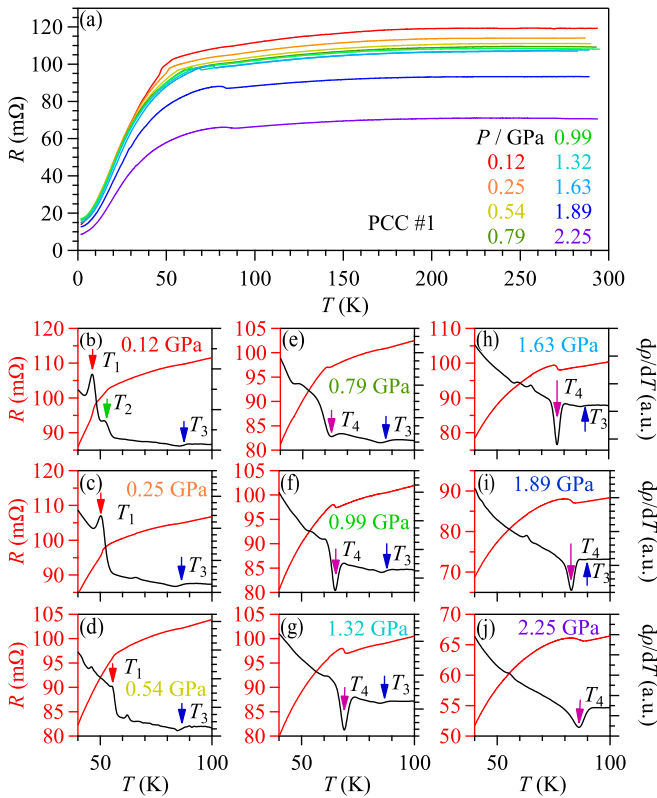


FIG. 2. (a) Temperature dependence of $R(T)$ under various pressures for NaMn₆Bi₅ (No. 1) in a PCC up to 2.25 GPa. (b)–(j) $R(T)$ and the corresponding dR/dT in the temperature range 40 to 100 K at different pressures. The arrows indicate different magnetic phase transitions.

palm-type cubic anvil cell (CAC) apparatus, which can maintain relatively good hydrostatic pressure conditions due to three-axis compression geometry [39,40]. The standard four-probe method was adopted with the current applied along the b -axis of the crystal. Liquid glycerol was employed as the PTM for the CAC. All the HP experiments in the PCC and CAC were performed in a ⁴He refrigerated cryostat with a 9-T superconducting magnet at the Synergic Extreme Condition User Facility, Huairou, Beijing [41]. For pressures > 15 GPa, the resistance $R(T)$ was measured in a BeCu-type diamond anvil pressure cell (DAC) with a 300- μ m culet. The four-probe method was adopted with soft KBr powder as the PTM, and the pressure was calibrated by the ruby fluorescent method at room temperature. The measurements with the DAC were performed in a ⁴He refrigerated cryostat and a commercial ³He refrigerator system down to 300 mK, respectively.

III. RESULTS AND DISCUSSION

Figure 1(b) shows $\rho(T)$ measured along the b -axis of single-crystal NaMn₆Bi₅ at AP. Upon cooling, $\rho(T)$ shows a metallic behavior and experiences a quick reduction around 50 K associated with the AFM transitions, which is a common feature of (K/Rb/Cs) Mn₆Bi₅ [33,37,38] and α -Mn [27,28]. A closer inspection of $\rho(T)$ around 50 K reveals two successive anomalies at about 46 and 52 K, as indicated by

the arrows in the inset of Fig. 1(b). In addition, there exists a third kink anomaly around 85 K. These anomalous features in $\rho(T)$ can be clearly defined from the $d\rho/dT$ curve, as shown in Fig. 1(c), from which we can determine precisely these three transition temperatures: $T_1 = 46$ K, $T_2 = 52$ K, and $T_3 = 85$ K. These results are consistent with those reported by Zhou *et al.* [36]. In addition to $\rho(T)$, the temperature dependence of magnetic susceptibility and specific heat also display discernable anomalies around these temperatures, confirming the bulk nature of these transitions. According to Ref. [36], the transitions at T_1 and T_2 have been ascribed to two AFM-like transitions, while the origin of the third transition at T_3 is still unclear. The presence of multiple phase transitions in NaMn₆Bi₅ distinguishes it from the other members, (K/Rb/Cs) Mn₆Bi₅ with a single AFM transition [33,37,38], and thus complicates the interpretation of the magnetic properties of AMn₆Bi₅. If we consider only T_1 and T_2 for NaMn₆Bi₅, the AFM transition temperatures follow the general trend of monotonic enhancement from ~ 50 K to 75 K, 83 K, and finally 87 K, with increasing the size of the A -site cation. According to the structural refinement results, replacing the A cations with a larger size mainly enlarges the interchain distances while keeping the [Mn₆Bi₅][−] chains almost intact. Then, the observed progressive enhancement of T_N upon inserting larger A -site cations should be ascribed to the weakening of the interchain coupling that would compete with the intrachain spin-spin interactions. That is, the larger interchain distances relieve the magnetic frustration between the inter- and intrachain interactions, giving rise to a higher T_N as observed.

To track the evolution with pressure of the aforementioned phase transitions, we first measured the resistance $R(T)$ of NaMn₆Bi₅ (No. 1) in fine intervals of pressure up to 2.25 GPa by using a PCC. All the $R(T)$ curves in the whole temperature range of 1.5 to 300 K are shown in Fig. 2(a), from which we can see an interesting crossover of the resistance anomaly around the AFM transitions. To see these features and their evolutions with pressure clearly, $R(T)$ in the temperature range 40 to 100 K together with the corresponding derivative dR/dT at each pressure were replotted in separate panels [Figs. 2(b)–2(j)]. The transition temperatures are clearly marked in these plots. As can be seen, three transitions marked by T_1 , T_2 , and T_3 are still visible at the first pressure of 0.12 GPa; the former two shift slightly to higher temperatures while the third one keeps nearly unchanged in comparison with those at AP. Upon increasing the pressure to 0.25 and 0.54 GPa, the transition at T_2 disappears and the peak anomaly at T_1 is reduced, yet shifts to higher temperatures progressively. With a further increase in pressure to 0.79 GPa, interestingly, $R(T)$ displays a weak upward anomaly around 60 K before changing the slope upon further cooling; this produces a dip in the corresponding dR/dT . Here, we labeled this transition temperature as T_4 to distinguish it from T_1 . The upward anomaly in $R(T)$ and the corresponding dip in dR/dT become pronounced and continuously move toward higher temperatures with pressure. It is noted that the upward step-like anomaly evolves into a hump-like one above 1.6 GPa. In this pressure range, the transition at T_3 is insensitive to pressure, and finally merges with $T_4 \approx 86$ K at 2.25 GPa. These results are reproduced in another sample (No. 2) and

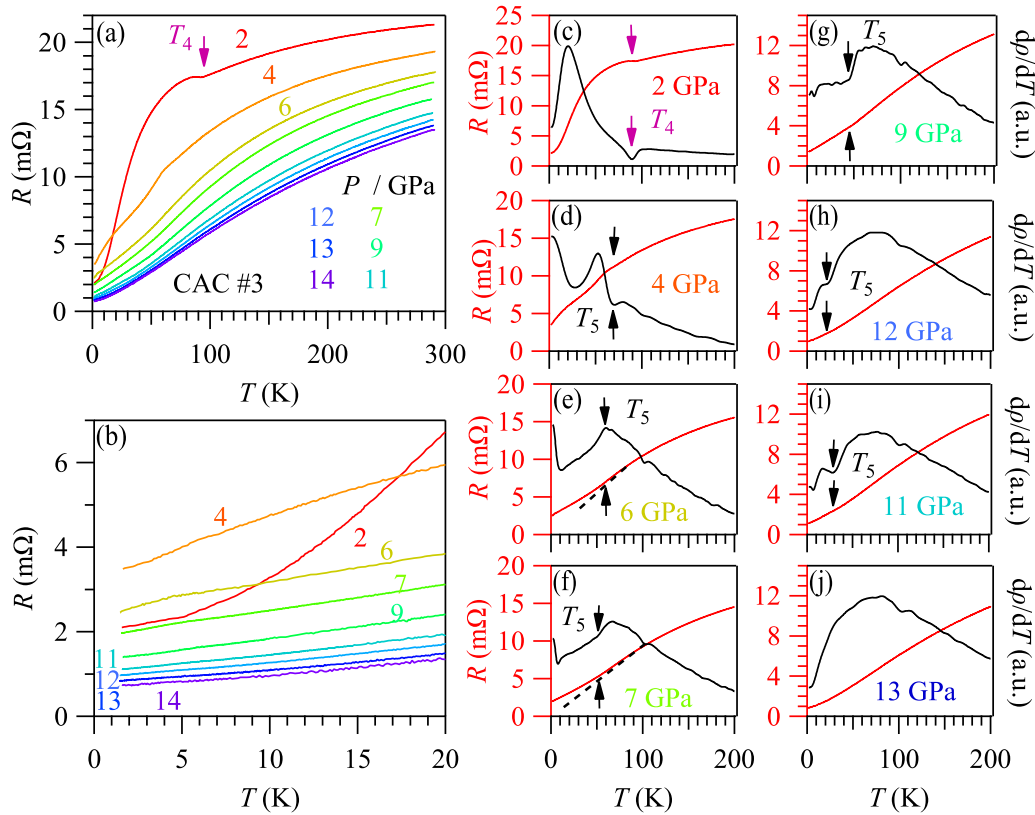


FIG. 3. Temperature dependence of $R(T)$ under various pressures up to 14 GPa in a CAC for NaMn_6Bi_5 (No. 3). (b) Low- T $R(T)$ ($1.5 \leq T \leq 20$ K). (c)–(j) $R(T)$ and the corresponding dR/dT in the temperature range 1.5 to 200 K at different pressures. The arrows indicate magnetic phase transitions.

demonstrate that the magnetic state of NaMn_6Bi_5 is so fragile that tens of kbar pressures can transform it into a new state characterized by a single transition like other AMn_6Bi_5 .

To monitor the evolution of the transition at T_4 , we then measured $R(T)$ of another NaMn_6Bi_5 (No. 3) single crystal under various pressures from 2 to 14 GPa by using a CAC. As shown in Fig. 3(a), the $R(T)$ at 2 GPa exhibits an upward hump-like anomaly around $T_4 \approx 90$ K, consistent with the previous results in PCC. When the pressure is increased to 4 GPa, however, the behavior of $R(T)$ is altered again; the up-turn disappears and a downward kink-like anomaly reemerges at a lower temperature, corresponding to a new peak in the dR/dT curve [Fig. 3(d)], labeled T_5 hereafter. At 4 GPa, a weak anomaly at T_4 remains visible. Upon further increasing the pressure to 6 GPa and above, the kink anomaly in $R(T)$ at T_5 is suppressed again and is gradually replaced by a very weak hump-like feature as shown in Figs. 3(e)–3(i). Eventually, this latter anomaly disappears completely at ~ 13 GPa [Fig. 3(j)], implying that the AFM order is suppressed completely by pressure. These $R(T)$ behaviors of NaMn_6Bi_5 in a CAC are very similar with those observed in (K/Rb) Mn_6Bi_5 [31,32]. To our surprise, however, we did not observe any sign of SC at temperatures down to 1.5 K and under pressures up to 14 GPa [Fig. 3(b)], in strikingly contrast with the (K/Rb/Cs) Mn_6Bi_5 that all show SC with T_c up to ~ 7 to 9 K in this pressure range.

We then adopted a DAC to measure the $R(T)$ of NaMn_6Bi_5 (No. 4, No. 5, and No. 6) single crystals at higher pressures.

The results are shown in Figs. 4(a)–4(c). The normal-state resistance decreases monotonously with pressure, but the characteristics of AFM transitions cannot be defined unambiguously due to the presence of nonhydrostatic pressure conditions in the DAC. Interestingly, we observed a slight drop of $R(T)$ starting at ~ 2 K in a limited pressure range (12 to 14.4 GPa), as marked by the arrows in Figs. 4(d)–4(f). Although the observed resistance drop is only $\sim 3\%$ to 25% of R_n , it is reproducible for all three samples, indicating that it is an intrinsic response of the sample. The discrepancies in the low-temperature $R(T)$ behaviors between the DAC and the CAC might be attributed to the different pressure conditions; the presence of stress and pressure gradient in the DAC should be responsible for the observed resistance drop.

The origin of this resistance anomaly is unclear at present, but it might be caused by the presence of some filamentary SC in analogy to other members of AMn_6Bi_5 . To check such a possibility, we loaded sample No. 6 in DAC into a ^3He refrigerator and recorded the $R(T)$ down to 0.3 K, as well as the $R(H)$ at different temperatures (0.30, 0.68, 1.06, and 1.44 K). As shown in Figs. 4(g) and 4(h), the resistance decreases by 10% down to 0.3 K and the application of external magnetic fields can restore the resistance drop gradually. Although this observation has been considered a common feature of SC, the absence of zero resistance suggests that the observed resistance drop, at most, corresponds to the emergence of filamentary SC. In addition, other possibilities

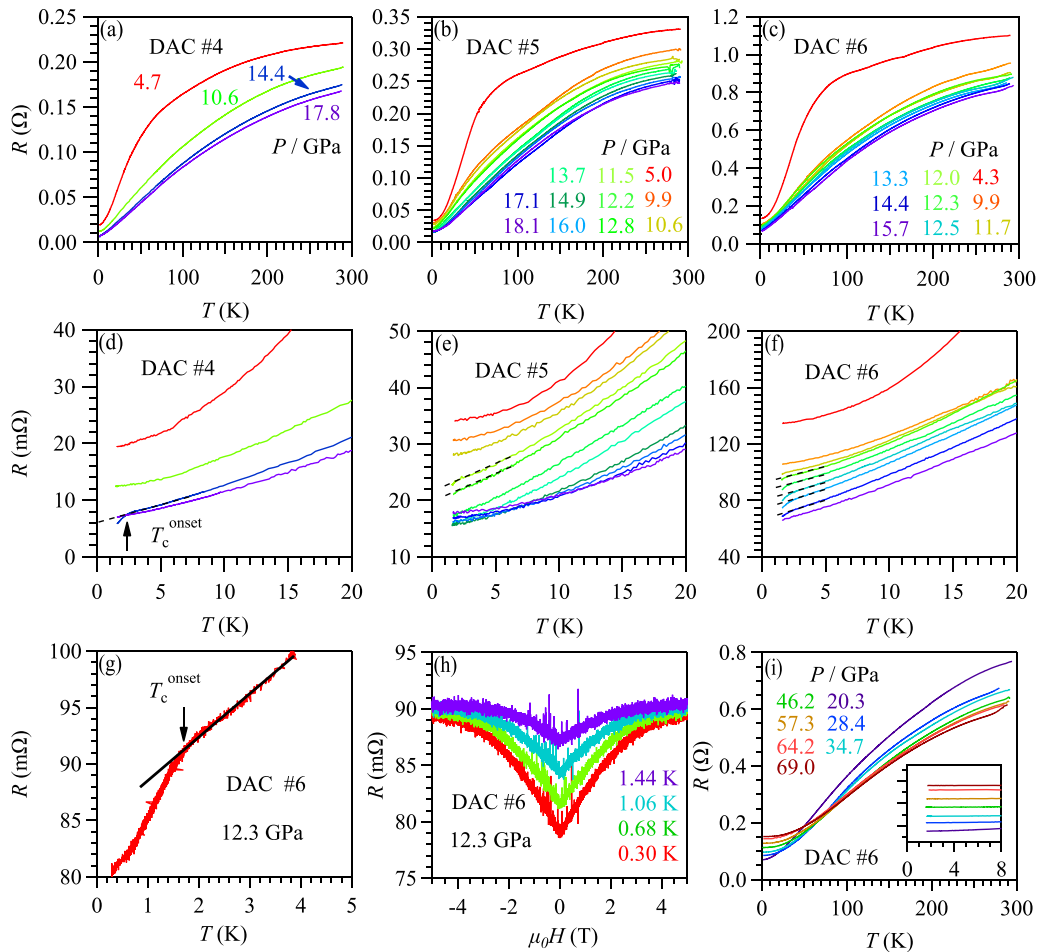


FIG. 4. (a)–(c) $R(T)$ of NaMn_6Bi_5 (No. 4, No. 5, No. 6) in a DAC under various pressures. (d)–(f) The enlarged view of $R(T)$ in the low-temperature range $1.5 \leq T \leq 20$ K. The dashed lines indicate that the resistance deviates from linearity, which can mark the T_c^{onset} . (g) Low- T $R(T)$ ($0.3 \leq T \leq 4$ K) at 12.3 GPa measured in a ^3He refrigerator. The T_c^{onset} is marked where the resistance deviates from linearity. (h) $R(H)$ at several selected temperatures of 0.30, 0.68, 1.06, and 1.44 K. (i) $R(T)$ of NaMn_6Bi_5 (No. 6) in a DAC up to 69 GPa.

such as the magnetic and other electronic phase transitions cannot be excluded by the present results. More studies are needed to unveil the origin of this anomaly. At the same time, the $R(T)$ of NaMn_6Bi_5 (No. 6) in a DAC was measured up to 69 GPa [Fig. 4(i)]. In the high-pressure range, there is no sign of SC. Our results demonstrate that the response to pressure of NaMn_6Bi_5 is unexpectedly different from that of (K/Rb) Mn_6Bi_5 .

Based on these results, a temperature-pressure phase diagram of NaMn_6Bi_5 was constructed. Figure 5 depicts explicitly how the multiple phase transitions evolve with pressure and then correlate to possible filamentary SC. As shown in Fig. 5, $T_1(P)$ increases with pressure and connects smoothly to $T_4(P)$ at ~ 0.8 GPa, which indicates that these two transitions should have a magnetic origin. The intermediate magnetic phase between T_1 and T_2 exists only at pressures below ~ 0.2 GPa. $T_4(P)$ continuously increases with pressure and merges together with the pressure-independent $T_3(P)$ at ~ 2 GPa, reaching a maximum of 90 K. At higher pressures, $T_5(P)$ decreases quickly and collapses completely at $P_c \approx 13$ GPa, where possible filamentary SC emerges at low temperatures within a quite narrow pressure range. For

(K/Rb/Cs) Mn_6Bi_5 , the superconducting dome covers a relatively broad pressure range of more than 10 GPa and the optimal T_c^{onset} reaches about 9 K, as mentioned earlier. In contrast, the solid evidence of SC is absent in the case of NaMn_6Bi_5 .

These comparisons thus distinguish NaMn_6Bi_5 from other members of AMn_6Bi_5 . The observed lower AFM transition temperatures in NaMn_6Bi_5 do not mean the presence of smaller localized magnetic moments or weaker spin-spin interactions. Instead, in the chemically precompressed NaMn_6Bi_5 , the interchain couplings are strengthened and compete strongly with the intrachain spin-spin interactions, which in turn can explain the lower AFM transition temperatures due to the magnetic frustration effect. The observed complex evolution of AFM transitions with pressure and the relatively higher critical pressure, P_c , in NaMn_6Bi_5 seem to be consistent with this scenario, i.e., the magnetic frustrations associated with strong interactions are relieved by higher pressures. Whether the enhanced magnetic frustrations are responsible for the absence of bulk SC in the chemically precompressed NaMn_6Bi_5 deserves further investigation.

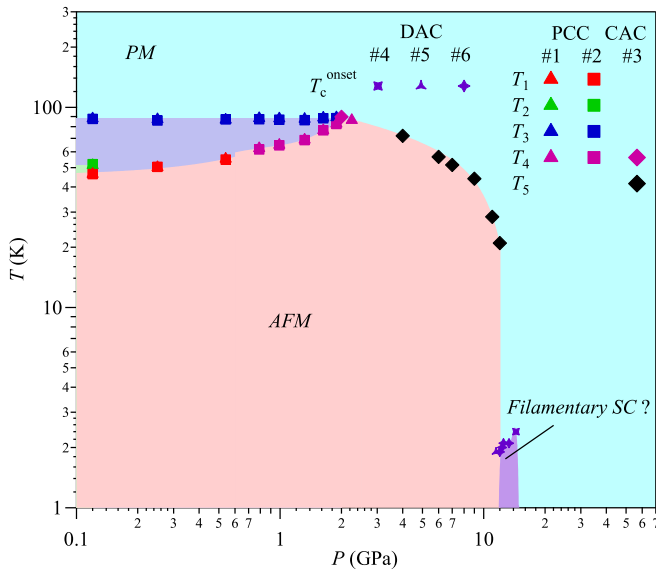


FIG. 5. Temperature-pressure phase diagram of NaMn_6Bi_5 . The pressure dependence of the magnetic transition temperatures (T_1 – T_5) and the T_c^{onset} are summarized.

IV. CONCLUSION

In summary, we carried out detailed electrical transport measurements on NaMn_6Bi_5 single crystals by using three different HP techniques. Our results not only reveal the

complex evolution of the multiple phase transitions upon compression, but also uncover the absence of bulk SC accompanying the collapse of AFM order. In comparison with AMn_6Bi_5 ($A = \text{K, Rb, Cs}$), the possible filamentary superconducting regime of NaMn_6Bi_5 is greatly reduced, and thus highlights the distinct magnetic characters of NaMn_6Bi_5 . As a complement to previous HP studies of the family of AMn_6Bi_5 [31–33], the present work provides more insights into the complex magnetism and its interplay with SC in this new class of Q1D manganese-based superconductors.

ACKNOWLEDGMENTS

This work is supported by the Beijing Natural Science Foundation (Grant No. Z190008), the National Key Research and Development Program of China (Grant No. 2021YFA1400200), the National Natural Science Foundation of China (Grants No. 12025408, No. 11921004, and No. 11834016), the Strategic Priority Research Program of Chinese Academy of Sciences (Grant No. XDB33000000), the CAS Interdisciplinary Innovation Team (Grant No. JCTD-2019-01), Lujiaxi international group funding of the K. C. Wong Education Foundation (Grant No. GJTD-2020-01), the Users with Excellence Program of Hefei Science Center CAS (Grant No. 2021HSC-UE008), and the Outstanding Member of Youth Promotion Association of CAS (Grant No. Y2022004). The high-pressure experiments were carried out at the Synergic Extreme Condition User Facility (SECUF).

- [1] J. G. Bednorz and K. A. Z. Mueller, *Z. Phys. B* **64**, 189 (1986).
- [2] P. A. Lee, N. Nagaosa, and X.-G. Wen, *Rev. Mod. Phys.* **78**, 17 (2006).
- [3] A. K. Saxena, in *High-Temperature Superconductors*, edited by A. K. Saxena (Springer, Berlin, 2012), p. 163.
- [4] Y. Kamihara, H. Hiramatsu, M. Hirano, R. Kawamura, H. Yanagi, T. Kamiya, and H. Hosono, *J. Am. Chem. Soc.* **128**, 10012 (2006).
- [5] Y. Kamihara, T. Watanabe, M. Hirano, and H. Hosono, *J. Am. Chem. Soc.* **130**, 3296 (2008).
- [6] H. Takahashi, K. Igawa, K. Arii, Y. Kamihara, M. Hirano, and H. Hosono, *Nature (London)* **453**, 376 (2008).
- [7] X. H. Chen, T. Wu, G. Wu, R. H. Liu, H. Chen, and D. F. Fang, *Nature (London)* **453**, 761 (2008).
- [8] Z. A. Ren and Z. X. Zhao, *Adv. Mater.* **21**, 4584 (2009).
- [9] K. Takada, H. Sakurai, E. Takayama-Muromachi, F. Izumi, R. A. Dilanian, and T. Sasaki, *Nature (London)* **422**, 53 (2003).
- [10] N. P. Ong and R. J. Cava, *Science* **305**, 52 (2004).
- [11] F. Steglich, J. Aarts, C. D. Bredl, W. Lieke, D. Meschede, W. Franz, and H. Schäfer, *Phys. Rev. Lett.* **43**, 1892 (1979).
- [12] Z. Ren, L. V. Pourovskii, G. Girit, G. Lapertot, A. Georges, and D. Jaccard, *Phys. Rev. X* **4**, 031055 (2014).
- [13] W. Wu, J.-G. Cheng, K. Matsubayashi, P. Kong, F. Lin, C. Jin, N. Wang, Y. Uwatoko, and J. Luo, *Nat. Commun.* **5**, 5508 (2014).
- [14] H. Kotegawa, S. Nakahara, H. Tou, and H. Sugawara, *J. Phys. Soc. Jpn.* **83**, 093702 (2014).
- [15] B. Keimer, S. A. Kivelson, M. R. Norman, S. Uchida, and J. Zaanen, *Nature (London)* **518**, 179 (2015).
- [16] J.-G. Cheng, K. Matsubayashi, W. Wu, J. P. Sun, F. K. Lin, J. L. Luo, and Y. Uwatoko, *Phys. Rev. Lett.* **114**, 117001 (2015).
- [17] Q. G. Mu, B. B. Ruan, B. J. Pan, T. Liu, J. Yu, K. Zhao, G. F. Chen, and Z. A. Ren, *Phys. Rev. Mater.* **2**, 034803 (2018).
- [18] J. K. Bao, J. Y. Liu, C. W. Ma, Z. H. Meng, Z. T. Tang, Y. L. Sun, H. F. Zhai, H. Jiang, H. Bai, C. M. Feng, Z. A. Xu, and G. H. Cao, *Phys. Rev. X* **5**, 011013 (2015).
- [19] Z. T. Tang, J. K. Bao, Y. Liu, Y. L. Sun, A. Ablimit, H. F. Zhai, H. Jiang, C. M. Feng, Z. A. Xu, and G. H. Cao, *Phys. Rev. B* **91**, 020506(R) (2015).
- [20] Z. T. Tang, J. K. Bao, Y. Liu, H. Bai, H. Jiang, H. F. Zhai, C. M. Feng, Z. A. Xu, and G. H. Cao, *Sci. China Mater.* **58**, 543 (2015).
- [21] Q. G. Mu, B. B. Ruan, B. J. Pan, T. Liu, J. Yu, K. Zhao, G. F. Chen, and Z. A. Ren, *Phys. Rev. B* **96**, 140504(R) (2017).
- [22] T. Liu, Q. G. Mu, B. J. Pan, J. Yu, B. B. Ruan, K. Zhao, G. F. Chen, and Z. A. Ren, *Europhys. Lett.* **120**, 27006 (2017).
- [23] Y. J. Li, W. Wu, K. Liu, Z. H. Yu, D. S. Wu, Y. T. Shao, S. H. Na, G. Li, P. Zheng, T. Xiang, and J. L. Luo, *Europhys. Lett.* **128**, 67002 (2020).
- [24] W. Wu, K. Liu, Y. Li, Z. Yu, D. Wu, Y. Shao, S. Na, G. Li, R. Huang, T. Xiang, and J. Luo, *Natl. Sci. Rev.* **7**, 21 (2020).
- [25] T. L. Hung, C. H. Huang, L. Z. Deng, M. N. Ou, Y. Y. Chen, M. K. Wu, S. Y. Huan, C. W. Chu, P. J. Chen, and T. K. Lee, *Nat. Commun.* **12**, 5436 (2021).

- [26] H. Kotegawa, M. Matsuda, F. Ye, Y. Tani, K. Uda, Y. Kuwata, H. Tou, E. Matsuoka, H. Sugawara, T. Sakurai, H. Ohta, H. Harima, K. Takeda, J. Hayashi, S. Araki, and T. C. Kobayashi, *Phys. Rev. Lett.* **124**, 087202 (2020).
- [27] T. Sato, K. Akiba, S. Araki, and T. C. Kobayashi, in *Proceedings of the International Conference on Strongly Correlated Electron Systems (SCES2019)*, edited by H. Takashi, and K. Takuro (JPS Conf. Proc., Okayama, Japan, 2020), p. 011030.
- [28] K. Akiba, K. Iwamoto, T. Sato, S. Araki, and T. C. Kobayashi, *Phys. Rev. Res.* **2**, 043090 (2020).
- [29] S. Sachdev, *Science* **288**, 475 (2000).
- [30] S. E. Sebastian, N. Harrison, C. D. Batista, L. Balicas, M. Jaime, P. A. Sharma, N. Kawashima, and I. R. Fisher, *Nature (London)* **441**, 617 (2006).
- [31] Z. Y. Liu, Q. X. Dong, P. T. Yang, P. F. Shan, B. S. Wang, J. P. Sun, Z. L. Dun, Y. Uwatoko, G. F. Chen, X. L. Dong, Z. X. Zhao, and J.-G. Cheng, *Phys. Rev. Lett.* **128**, 187001 (2022).
- [32] P. T. Yang, Q. X. Dong, P. F. Shan, Z. Y. Liu, J. P. Sun, Z. L. Dun, Y. Uwatoko, G. F. Chen, B. S. Wang, and J.-G. Cheng, *Chin. Phys. Lett.* **39**, 067401 (2022).
- [33] S. J. Long, L. Chen, Y. X. Wang, Y. Zhou, S. Cai, J. Guo, Y. Z. Zhou, K. Yang, S. Jiang, Q. Wu, G. Wang, J. P. Hu, and L. L. Sun, *Phys. Rev. B* **106**, 214515 (2022).
- [34] J. K. Bao, H. Cao, M. J. Krogstad, K. M. Taddei, C. Shi, S. Cao, S. H. Lapidus, S. van Smaalen, D. Y. Chung, M. G. Kanatzidis, S. Rosenkranz, and O. Chmaissem, *Phys. Rev. B* **106**, L201111 (2022).
- [35] M. Tinkam, *Introduction to Superconductivity* (Dover Publications, Mineola, NY, 1996).
- [36] Y. Zhou, L. Chen, G. Wang, Y. X. Wang, Z. C. Wang, C. C. Chai, Z. N. Guo, J. P. Hu, and X. L. Chen, *Chin. Phys. Lett.* **39**, 047401 (2022).
- [37] J. K. Bao, Z. T. Tang, H. J. Jung, J. Y. Liu, Y. Liu, L. Li, Y. K. Li, Z. A. Xu, C. M. Feng, H. Chen, D. Y. Chung, V. P. Dravid, G. H. Cao, and M. G. Kanatzidis, *J. Am. Chem. Soc.* **140**, 4391 (2018).
- [38] L. Chen, L. Zhao, X. Qiu, Q. Zhang, K. Liu, Q. Lin, and G. Wang, *Inorg. Chem.* **60**, 12941 (2021).
- [39] Y. Uwatoko, K. Matsubayashi, T. Matsumoto, N. Aso, M. Nishi, T. Fujiwara, M. Hedo, S. Tabata, K. Takagi, M. Tado, and H. Kagi, *Rev. High Pre. Sci. Tech.* **18**, 230 (2008).
- [40] J.-G. Cheng, K. Matsubayashi, S. Nagasaki, A. Hisada, T. Hirayama, M. Hedo, H. Kagi, and Y. Uwatoko, *Rev. Sci. Instrum.* **85**, 093907 (2014).
- [41] J.-G. Cheng, B. S. Wang, J. P. Sun, and Y. Uwatoko, *Chin. Phys. B* **27**, 077403 (2018).